VERY HIGH FIELD HYBRID MAGNET SYSTEMS

D. Bruce Montgomery, J.E.C. Williams,* N.T. Pierce,
R. Weggel, and M.J. Leupold

Francis Bitter National Magnet Laboratory†
Massachusetts Institute of Technology
Cambridge, Massachusetts

I. GENERAL CONSIDERATIONS

The term "hybrid" magnet has been coined to describe coils in which only part of the field is generated by superconductors and part by nonsuperconductors. Such systems have the advantage that they can produce higher fields than can be produced by either of their parts alone. In addition, they can represent a rather economical approach to very high fields for laboratories who already possess either power supplies or refrigerators of reasonable capacity.

The most compelling reason to consider hybrid systems is that superconductors by themselves are limited by their upper critical field. If one wants to produce a field above this level, it is clear that the superconductor cannot do it alone. If, on the other hand, we replace those sections of the winding which are exposed to a field too high for the superconductor by nonsuperconducting materials, we can go on increasing the field limited only by our ability to power or cool the now dissipative inner regions. Needless to say, one must separate the two sections by a suitable cryostat. This cryostat must not only provide low loss temperature isolation, but must support very large magnetic interaction forces as well.

When one designs an actual hybrid system it is necessary to take a more subtle approach than simply replacing only those windings which would be above the upper critical field of the superconductor. One needs to take into account the power (or cryogenic cooling) available, the space required for the nonsuperconducting insert, and the cost of the superconducting magnet as a function of field and bore.

Let us first consider the relative cost of superconducting magnets as a function of field. This will give us an indication both of how high field a superconducting coil we will be willing to invest in for the hybrid, and at the same time indicate what practical upper limits of field we might expect from an all superconducting system.

It is well known that the current carrying capacity of superconductors drops rapidly as the critical field is approached. Figure 1 shows the critical current for a widely used commercial Nb_3Sn material nominalized to that at 100 kG for 4.2°K[1] and for 1.5°K.[2] If we wish our conductor to carry a fixed current, the amount of Nb_3Sn which must be used in the conductor must increase as the inverse of Fig. 1. As the conductor price is related almost directly to the amount of Nb_3Sn, we can construct a relative cost curve as in Fig. 2. We have added as well the relative cost of NbTi in the low field region as it becomes less costly than Nb_3Sn.

---

*Present address, Oxford Instrument Co. Ltd., Oxford, England.

†Supported by the U.S. Air Force Office of Scientific Research.

1. RCA Nb_3Sn ribbon R60291 $0 < H < 140$ kG; above 140 kG data from D.B. Montgomery and W.B. Sampson, Appl. Phys. Letters 6, 108 (1965).

2. W.B. Sampson, private communication.

To compute the relative cost of magnets from Fig. 2 we must make assumptions about the amount of material per unit volume of the magnet which requires that we settle on the number of subdivisions, current density, and on the number of turns/cm^2. For small bore, high field coils reasonable current density and turns/cm^2 to assume are given in Fig. 3 and are based on adding Nb_3Sn to maintain constant current and adding copper in proportion to the linearly increasing magnetoresistance.

Figure 4 plots the relative cost of 1.5 inch bore, all superconducting magnets under the assumptions discussed for various numbers of subdivisions of the coil. It is clear that costs rise extremely rapidly at high fields, even at reduced temperatures. We might expect from such a figure to see hybrid systems considered for any fields above 175 kG, and certainly for all fields at 200 kG or higher. While future materials may alter these dividing points somewhat, the fact remains that there will always be a dividing point at which it is advantageous or necessary to consider hybrids.

As an indication of materials to come, Fig. 1 also gives the critical current density of some V_3Ga material[3] in its absolute relation to that of Nb_3Sn at 4.2°K. Its probable performance at 1.5°K should make it the best available material for this very high field range.

Superconducting coils for use in hybrid systems must, of course, have much larger bores than those in Fig. 4, but will be subject to the same steep rises in costs as fields increase. Figure 5, for example, indicates the relative cost of a 10 in. room-temperature bore superconducting system relative to the cost at 50 kG. Cryostat and power supply costs have been included in this case, and the relative cost of material is based on Fig. 2 and an assumed current density of 5×10^3 A/cm^2. We note that the system costs at 120 kG is nearly twice what it is at 100 kG.

It is of interest to examine the magnitude of the absolute costs of this 10 in. system. If we tie Fig. 2 to a typical figure for cost per ampere per meter at today's prices we can calculate the material costs. If we take \$16.50 per kA/m at 100 kG we obtain a material cost for the 12 in. 50 kG superconducting coil (10 in. room-temperature bore) of \$30 000 and with the \$20 000 additional system cost get a normalizing nonsalary cost for Fig. 5 of \$50 000 at 50 kG. In addition, one would need to add engineering and labor costs which can easily be equal to material costs in prototype systems. Taking the nonsalary figure of \$50 000 at 50 kG we thus note that a 100 kG system is worth \$150 000 in material costs alone and a 120 kG system, \$265 000. We are therefore talking about major investments and we see that we are unlikely to wish to exceed 100 kG by very much in the superconducting part of the hybrid.

Let us now shift our attention to the nonsuperconducting insert. This can be a water-cooled coil or a cryogenic coil and which one to choose depends on a number of variables. Probably the most important factor is what is already available to the designer. Most of the larger high energy physics laboratories, for example, can make at least several megawatts of power available as can any of the laboratories already engaged in high field water-cooled magnet work. Some facilities, on the other hand, have large cryogenic capacity and a shortage of power. If one is starting from the beginning with nothing available, the problem is more complex and the decision is often most heavily influenced by what else might be done with the facility were it available.[4] In this paper we will restrict our attention to water-cooled inserts as we already have considerable dc power and the need for many hours of continuous fields.

---

3. Ribbons made by K. Tashikawa, National Research Institute for Metals, Tokyo, and tested at the Francis Bitter National Magnet Laboratory by Y. Iwasa.

4. R. Stevenson and P. Marston, Colloque international sur les champs magnétiques intenses, Grenoble, 1966 (CRNS, Paris, 1967), p. 169.

We will start our discussion by considering what fields one might expect to achieve given a 100 kG superconducting coil of sufficient size to accommodate water-cooled coils at various power levels. This is shown in Fig. 6. With 2 MW we can achieve 200 kG in a 1.5 in. bore coil (1.25 in. working bore) and with 4 MW, 250 kG. Above a field of 250 kG the insert itself begins to suffer from some of the same limitations of critical current that affect superconductors, namely that the magnetic stresses are becoming so high that performance begins to suffer. The coil must either use increasingly strong conductors or give up increasing space to support structure. The power required per gauss therefore goes up. We have therefore shown the curve in Fig. 6 dividing above 250 kG; the upper curve represents an ideal situation of no limitation, and the lower one, the more practical case. Nonetheless, we note that with 10 MW one can achieve a field of over 300 kG.

We next examine how large a superconducting coil we need to build for a given hybrid system. The minimum size is dictated by the smallest bore large enough to contain a coil able to dissipate the power we wish to use. This is generally not the optimum size, however, as we shall discuss. Let us assume that we wish to generate 200 kG in a 1.25 in. bore and we have 2.5 MW of power available. We would first proceed to calculate the field that an insert of 1.5 in. inside diameter would produce as a function of its outer diameter. As the insert coil is enlarged, the gauss per watt goes up due to the increase in the coil's Fabry factor and the decrease in operating temperature. The increase in insert field with outer diameter means that less field need be generated by the superconducting coil to reach 200 kG, but also requires that the superconducting coil have a progressively larger bore to accommodate the larger insert. It is thus necessary to examine the balance between the cost of increasing the bore against that of producing a higher field at a smaller bore. Figure 7 shows the results for this case and for a 5 MW, 250 kG case. We note that there is an insert coil outer diameter which yields a minimum cost system at the given power and required field. Where the minimum will lie depends upon the type of insert, the power level, the field range and the cost of the superconductor. The minimum can thus be expected to shift with changing economics of the superconducting material. Figure 7 is given only to indicate that there will be an optimum size to pick and that within plus or minus one to two inches, it is not particularly critical.

Having found the optimum, it is necessary to go back and be sure that it is feasible to build a coil within that optimum space which can be supported and cooled. This is a more complex question as there is seldom an absolute limit on performance. A pair of typical insert coils are shown in Fig. 8 to give an indication of what is possible. The insert coil has an i.d. of 1.5 in. and an o.d. of 4.375 in. and absorbs 1.1 MW to generate 75 kG. It could easily absorb 1.5 MW. The second coil of 4.6 in. i.d. and 13 in. o.d. absorbs 5 MW and generates 100 kG. The over-all diameter outside the retaining structure is 14 in. A proposed future coil system has been designed to absorb 16 MW within the same envelope although with a different coil arrangement. Based on our experience with coils like these we feel that the minimum allowable size will generally fall below the optimum size, particularly if multiple coil arrangements are used.[5]

A 10 in. room temperature bore superconducting coil as discussed in connection with Fig. 5 would be close to the optimum size for a 2.5 MW insert, and if it generates 90 kG would give a 200 kG central field. This coil would represent an investment of about $120 000 exclusive of salary costs and would be considerably less costly than the all-superconducting coils indicated in Fig. 4. As the field required increases further, hybrids must be used and the question is no longer one of economics.

---

5. D.B. Montgomery, Colloque international sur les champs magnétiques intenses, Grenoble, 1966 (CRNS, Paris, 1967), p. 51.

II. PROTOTYPE HYBRID MAGNET

1. Over-all System

We are constructing a prototype hybrid system which will use various water-cooled insert coils in a 14 in. room temperature bore 60 kG superconducting coil. Total fields of 225 kG in a 1.25 in. bore or 200 kG in a 2.125 in. bore can be produced for 5 MW of power input. Later inserts at 10 and 16 MW can be expected to produce fields close to 300 kG. While it appears technically and economically feasible to construct outer coils up to 120 kG, the lower field prototype was selected to remain within the convenient range of NbTi and to minimize coil development problems. As we shall discuss, there are a number of severe problems which must be met in connection with the cryostat design, as well as an immediate need for the system in the magnet facility; we therefore considered it expedient to choose a superconducting coil of modest performance. Before discussing the design details of the superconducting coil, we shall examine the over-all system and the cryostat design.

Figure 9 shows the over-all system, which consists of the superconducting magnet cryostat, external 250 liter storage vessel, 8 kW power supply, and a typical water-cooled insert. The storage cryostat is considered a permanent part of the system and is connected to the magnet cryostat by a permanently installed, shielded, low loss transfer tube. Helium can be transferred into the magnet cryostat for operation and the excess out again after the run. Between runs the coil will be held at 20°K by a small regenerative refrigerator.[6]

The power supply can charge the 2 MJ superconducting magnet in 15 minutes and sweeping operation will then be accomplished by the insert. An energy removal protective system parallels the coil by a permanently installed 0.1 Ω resistor and disconnects the protected power supply by means of a two-pole breaker.

When additional hybrid systems become operational in the laboratory, it is proposed to connect them all together with a 500 W helium refrigerator.

2. Magnet Cryostat

The superconducting magnet cryostat and the two-coil water-cooled insert are schematically shown in Fig. 10. The insert is similar to that pictured in Fig. 8. All water and power connections are located at the bottom and the 14. in. o.d. retaining structure and coils can be easily removed as a unit up through the open bore of the magnet cryostat without disturbing the cryostat. Any other standardized insert can then be reintroduced, all without any necessity of warming up the superconducting coil.

The magnet cryostat can be very short as it needs to contain no reservoir of helium, the helium being supplied from the external storage vessel. The helium cryostat is welded shut to avoid seal problems and is suspended from supports at 77°K by 1/8 in. diameter stainless-steel cables running from the bottom of the helium cryostat to the top of the nitrogen cryostat and vice versa. A nitrogen shield cryostat is used rather than a gas cooled shield because of the desire to hold the coil at 20°K when no helium is present; the nitrogen reduces the load that the 20°K refrigerator must supply. The nitrogen cryostat and vacuum vessel are aluminum, the radiation shields copper, and the helium cryostat stainless steel. Cooldown weight of the coil and helium cryostat is 2000 lb.

---

6. W. Hogan and R.W. Stuart, Cryodyne Refrigerator, ASME 63-WA (1963) by A.D. Little, Inc.

Access to the helium cryostat is provided through a 40 in. long 3 in. diameter stack tube. This allows the use of long counter flow leads[7] and minimizes the neck tube loss. The leads may be remotely disconnected near the top of this stack and the low temperature side of the disconnect is shielded from heat input by a separate vacuum space. The leads will remain connected during operation as no persistent operation is possible (due to coupling with the changing field of the copper coil), but will be disconnected between runs to minimize heat input which must be removed by the 20°K refrigerator.

The principal design problem which must be met in the magnet cryostat is the support of the magnetic interaction forces between the insert and superconducting coil. The interaction forces, calculated on an inductance basis, result in an axial spring constant of 40 000 lb/in. and a radial spring constant of 6000 lb/in. of radial displacement. Under ordinary conditions the axial force is a restoring force and, by proper alignment and the allowance of some relative axial motion, would not be troublesome. However, during assymmetric failure of the copper coil, the magnetic centers would be displaced and a large accelerating force would be introduced. While these conditions will only exist during the 300 msec period required to fully open the breakers, the peak accelerating force can reach 24 g. The axial support cables running from the helium cryostat to the nitrogen cryostat, and from the nitrogen cryostat to the vacuum vessel, contribute an effective spring constant of 10 000 lb/in. and under higher off-center loads, stretch elastically to allow the inner cryostat to come up against stops (not shown in the figure) carried by the upper and lower radiation shield covers. They thus transfer the loads directly to the vacuum vessel covers. The vacuum vessel (and the insert magnet assembly) are both mounted on stiff spring systems and can then move to reduce the off-center loads. The coil is held inside the helium cryostat by long bolts passing through a cover plate above the coil and threaded into the cryostat base plate.

The radial forces are unstable and it is therefore necessary to have a restoring radial spring constant in the cables greater than the upsetting magnetic spring constant. A restoring spring constant of 15 000 lb/in. is provided. Radial cables running from the helium to the nitrogen cryostat are fixed in place, while those running from the nitrogen cryostat to the vacuum vessel are externally adjustable to minimize forces by proper initial alignment. Experience with the first system will indicate if this adjustment feature is necessary.

The estimated helium losses for the cryostat under various conditions, as well as cooldown requirements, are given in Table I.

3. The Superconducting Coil

A. Coil construction. The design parameters for the superconducting coil to be used with the prototype hybrid system are given in Table II. The coil is to be constructed from 24 double pancakes, with each double pancake wound from a single 620 ft piece of 0.079 in. × 0.397 in. copper NbTi composite material.[8] The specified conductor parameters are given in Table III.

The turns of the pancakes are separated by 0.1 in. long by 0.015 in. high polyester-glass spacers which are cemented in place by a silicone adhesive coating on both

---

7. K.R. Efferson, Rev. Sci. Instr. 38, 1776 (1967).

8. The composite material was manufactured by Cryomagnetics, Inc. Denver, Colorado.

TABLE I

Estimated Cryostat and Cooldown Losses

1. Input to helium cryostat (4.2 - 77°K)	
Axial cables	0.04 W
Centering cables	0.17 W
Neck tube	0.10 W
Radiation (emissivity = 0.05)	0.21 W
	0.52 W ≅ 750 x 10^{-3} liter/h
Lead losses at 1500 A	3.0 W ≅ 4.2 liter/hr
2. Input to nitrogen cryostat	
Axial cables	0.6 W
Centering cables	2.4 W
Radiation (0.25 in. superinsulation)	9.3 W
	12.3 W ≅ 0.27 liter/h
3. Helium cooldown requirements (perfect exchange conditions)	
To cool from 77°K	140 liter
To cool from 70°K	115 liter
To cool from 20°K	5 liter

TABLE II

Coil Parameters

Inside diameter	16 in.
Outside diameter	26 in.
Length	23 in.
Number of double pancakes	24
Number of turns per pancake	52
Length of individual conductors (single length per double pancake)	610 ft
Total conductor length	14 700 ft
Coil weight	1500 lb
Internal cooling passages	0.017 in. x 0.3 in. (75% of internal surface)
Edge cooling	80% of each pancake face
Central field	60 kG
Maximum winding field	65 kG
Design current	1500 A
Maximum fault current	1650 A
Energy storage	2 x 10^6 J

TABLE III

Conductor Parameters

Cross section	0.397 in. x 0.079 in. (10 mm x 2 mm)
Ratio of copper to superconductor	8:1
Number of superconducting strands	60
Diameter of superconducting strands	≈ 0.0091 in.
Exposed surface/cm length	2.25 cm^2
Anticipated resistivity at 65 kG	3.75 x 10^{-8} Ω·cm
Stability parameters (Fig. 16)	α_n = 0.25, β_n (4.2°K) = 0.3
Maximum heat flux (1650 A)	0.25 W/cm^2

sides of 0.001 in. Mylar tape.[9] The bond will resist a modest force of 100 lb at 77°K applied parallel to the tape surface per square inch of bond surface. The faces of each pancake are fully exposed for cooling with the exception of 64 0.2 in. wide radial Micarta spacer strips which separate the pancakes and support the axial forces. They cover 15% of the face cooling surface. The integrated axial compression force at the mid-plane is 300 000 lb, giving a compressive force on the insulator strip of 5500 psi.

The pancakes are banded at the outer diameter by a yellow brass tension band 0.187 in. thick, closed by a half inch bolt. The yellow brass has a yield strength of 45 000 psi at 300°K and an integrated contraction[10] higher than that of copper ($\Delta L/L = 397 \times 10^{-5}$ from 300°K to 0°K).

The peak conductor stress is 10 800 psi distributed across the conductor and the resultant strain is so small that no adverse effect on resistivity is anticipated. The thermally induced stress resulting from the differential contraction of copper and NbTi for the 8:1 copper-to-superconductor ratio composite adds an additional 2500 psi (see Fig. 15).

All connections are at the outside of the coil and are overlapped, soldered, and bolted to a support structure. The pancakes are wound on a removable mandrel and are thus not wound on a core tube. The cross-over turn from one half of the pancake to the other is supported by appropriately placed insulated pieces.

B. Choice of conductor and anticipated coil performance. In view of the potential problems associated with the cryostat and operation of the prototype system it was decided to build as conservative a coil as possible. The coil is expected to be fully stable (that is, have a recovery current higher than the operating current) and to operate at a relatively modest current density of 5×10^3 A/cm^2. To specify and select an appropriate conductor, a number of tests on magneto- and stress-induced resistivity, thermal stresses, heat transfer, thermal conductivity, and finally voltage-current characteristics of short samples were undertaken.

i) Heat flux measurements. A test was made to determine the take-off and recovery heat fluxes for the conductor and passage geometry to be used in the coil. A 0.25 W carbon resistor was embedded in a 1 cm wide copper conductor backed with a stainless-steel heater strip. The conductor was then spaced off a vertical plate by the 0.017 in. insulator strips to be used in the coil, and the heater strip side blocked off from effective contact with the helium. The results are shown in Fig. 11. The recovery heat flux of 0.31 W/cm^2 can be further reduced to 0.25 W/cm^2 if sufficient additional heat is put into a heater below the test section, choking the passages with bubbles. It is clear that the most conservative approach would limit the heat flux with all the current in the copper to 0.25 W/cm^2, and this we have done.

We have selected a passage height of 0.017 in. as a reasonable compromise between overly restricting heat flux and reducing the packing fraction. The influence of changing the passage height on the total conductor required is shown in Fig. 12 insofar as the passage height changes the turns/cm^2 and hence the over-all current density at fixed current. We note that the coil size and conductor thickness make the influence of passage size on conductor length rather small.

ii) Stress and resistivity. In order to anticipate what reasonable value of resistivity to expect for the conductor a series of tests was undertaken. Magnetoresistance data taken on magnet wire and five NbTi copper composites are summarized in Fig. 13.

---

9. Mylar double coated "Scotchpar," 3M Company Tape No. Y930.

10. R.B. Scott, Cryogenic Engineering (Van Nostrand, Princeton, N.J., 1959).

We note that the slopes of all the curves are very similar and that only the materials of a resistivity less than the 100:1 deviate appreciably from a linear relationship. Once knowing the initial resistivity and the slope one can estimate rather well the operating resistivity.

Also shown in Fig. 13 is the relationship between stress-induced resistivity and magnetoresistance. Curves 1 and 2 and curves 7 and 8 represent two samples before and after strain. The curves simply move up and consequently can also be constructed from zero field strain-resistivity measurements and zero strain magnetoresistance measurements. The magnetoresistance measurements in Fig. 13 were taken at 12°K so that resistivity of the copper could be measured in the presence of superconductors in the composite.

The effect of strain on zero field resistivity for annealed magnet wire is shown in Fig. 14. It is interesting to note that most of the strain-induced resistivity introduced at low temperature in copper anneals out upon returning to room temperature.

Stress can be introduced both by magnetic forces and by thermal contraction. The thermally induced stress in a NbTi copper composite (assuming zero stress at 300°K) is shown in Fig. 15 as a function of the ratio of copper to superconductor. The figure is based on a measured[11] modulus at 4.2°K of $E = 12.2 \times 10^6$ for NbTi and $E = 20 \times 10^6$ for copper, and a measured[11] 300°K to 77°K integrated contraction of $\Delta L/L = 131 \times 10^{-5}$ for NbTi and $\Delta L/L = 310 \times 10^{-5}$ for copper. For large copper-to-superconductor ratios, the stress is small, and little effect on resistivity from thermal contraction alone would be expected above a ratio of 2 to 1.

iii) Stability. Having explored allowable heat fluxes and expected resistivities, it is possible to specify the desired characteristics of the composite in regard to the ratio of copper to superconductor and the number of strands of superconductor. The parameters of the composite chosen for our 60 kG coil are given in Table III.

The stability parameters are defined in Fig. 16. It will be noted that the usual stability parameter,[12] α, has to be redefined as α_n to allow the use of a nonlinear heat transfer coefficient. We have also introduced a second parameter, β_n, relating to the temperature rise associated with thermal gradients within the superconductor. The simple model used assumes a uniform distribution of current within the superconductor and a mean temperature rise given by Eq. (4), Fig. 16. The influence of α_n and β_n can be combined into a single stabilization equation[13] as given in Fig. 16.

We can demonstrate the effect of α_n and β_n on stability by the use of Fig. 17 and Fig. 18. Figure 17 assumes $\beta_n = 0$ and shows only the effect of the nonlinear heat transfer which is assumed to be of the sample form of Eq. (1), Fig. 16, with $h_o = 4$, $n = 2$. One notices discontinuities at $I = I_c$, an occurrence which has been reported previously.[14] Figure 18 assumes a fixed value of $\alpha_n = 0.25$ and shows the effect of gradients in the superconductor. These gradients can also introduce discontinuities at $I = I_c$. One must therefore know something about the thermal conductivity of the superconductor, and should then choose N to limit the discontinuity of the critical

---

11. Measured at the Francis Bitter National Magnet Laboratory by N.T. Pierce and C. Park.

12. Z.J.J. Stekly and J.L. Zar, IEEE Trans. Nucl. Sci. NS-12, No. 3, 367 (1965).

13. D.B. Montgomery, Magnet Design (John Wiley & Sons, New York, 1969), Chap. 6.

14. W.F. Gauster and J.B. Hendricks, in Proc. IEEE Intermag Conference, Washington, 1968 (to be published).

current chosen. (For a fixed current, if N gets larger, the strand diameter must get smaller.)

The thermal conductivity of NbTi at H = 0 is given[15] in Fig. 19 and is a rapidly changing function of temperature. (In Fig. 18, the conductivity is assumed fixed and if taken at the 4.2°K value, for example, will obviously overemphasize the effect.) To assure no discontinuity we chose a large number of individual conductors, N being 60 for our composite.

---

15. These measurements were made by A. Milner and R. Hale at the Francis Bitter Magnet Laboratory. The material was supplied by Cryomagnetics, Inc., Denver, Colorado.

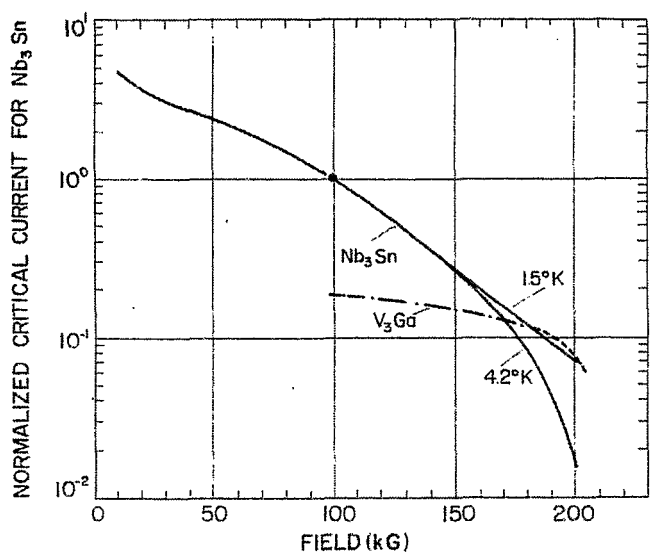

Fig. 1. Critical currents for Nb_3Sn ribbons at 4.2°K (Ref. 1) and 1.5°K (Ref. 2) as a function of field, normalized to their values at 100 kG. Also shown is a sample of V_3Ga (Ref. 3) at 4.2°K in its absolute relation to Nb_3Sn at 4.2°K on the basis of equivalent over-all cross section.

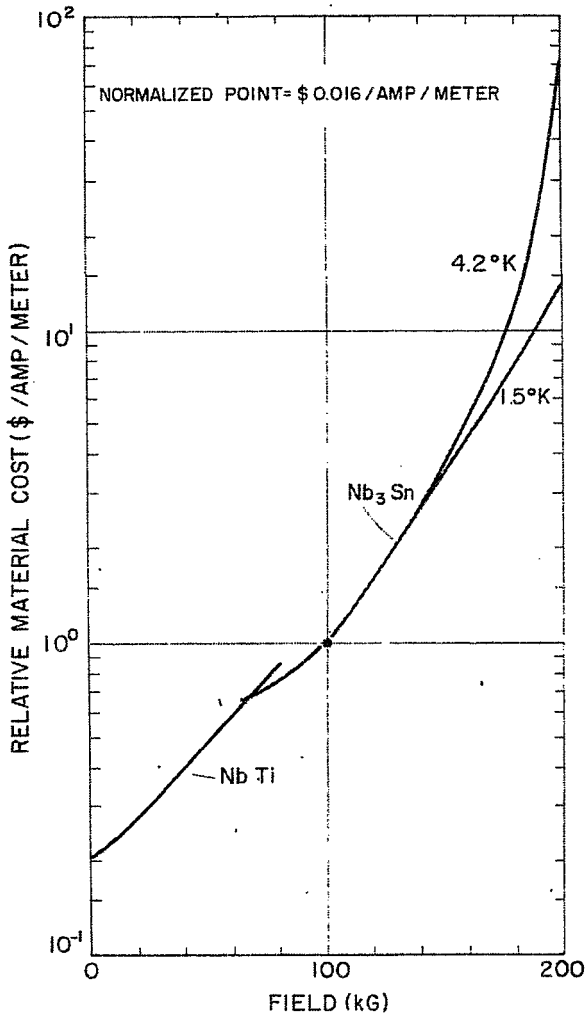

Fig. 2. Relative cost of NbTi and Nb_3Sn at 4.2°K and 1.5°K based on Fig. 1 and the assumption that cost is inversely related to current at fixed field. The curves have been normalized to 1 at 100 kG where current prices indicate an average approximate cost of $16.50 per kA/m.

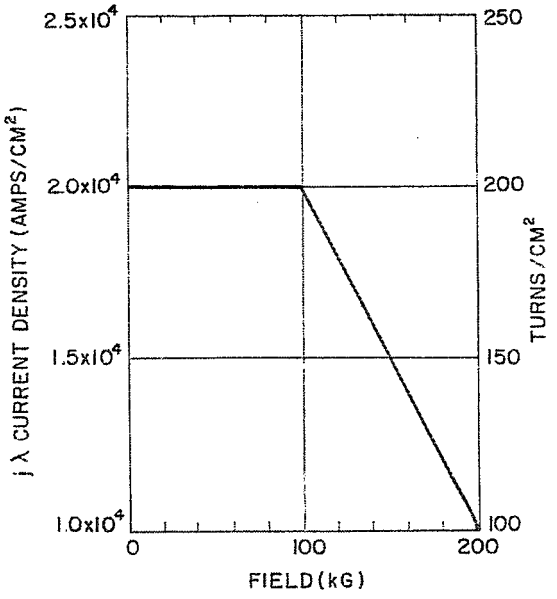

Fig. 3. Assumed over-all current density and turns/cm^2 used with Fig. 4.

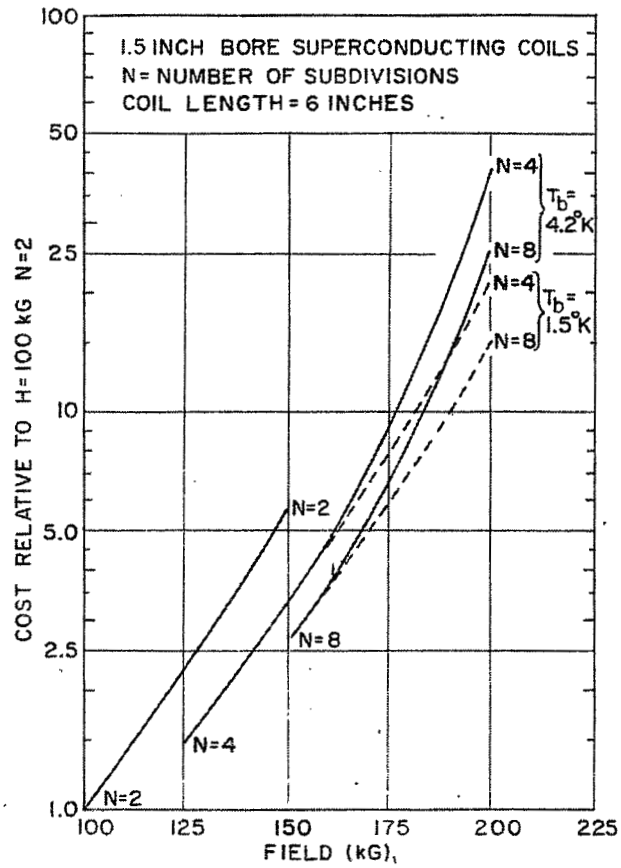

Fig. 4. Cost of 1.5 in. bore superconducting coils in relation to costs at 100 kG. The number N is the number of subdivisions of the coil. Each subdivision, starting at the inside, is assumed to produce a field h_1 = 1 unit, h_2 = 2 units ... , h_n = n units, thus generating progressively more field with the lower field coils. Curves are shown for 4.2°K and 1.5°K. We note that the cost of 200 kG coils ranges from 15 to 40 times costs at 100 kG.

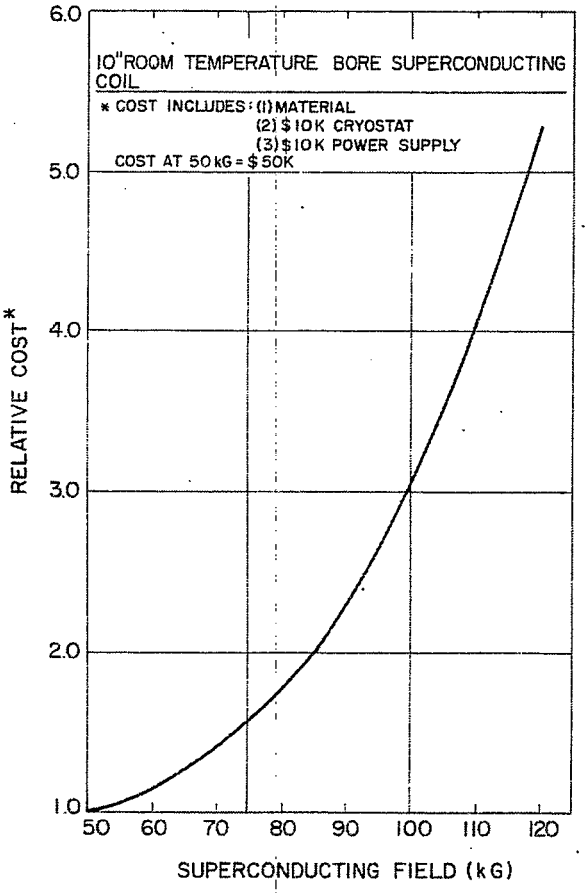

Fig. 5. Relative cost of a 10 in. room temperature bore (12 in. i.d.) superconducting coil as a function of field. The normalized cost at 50 kG includes $10 000 for a cryostat and $10 000 for a power supply and $30 000 for materials. No construction costs are included.

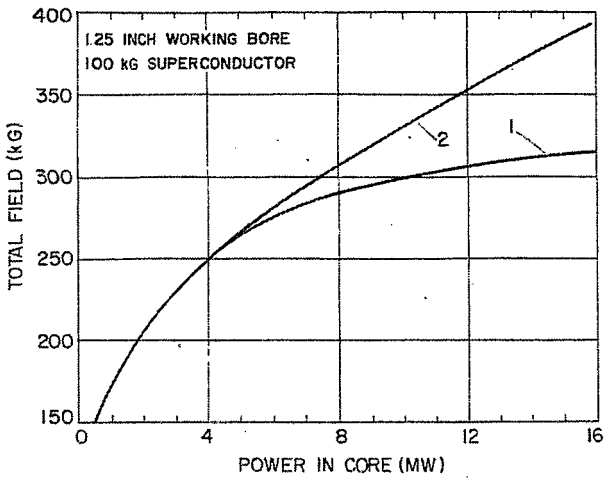

Fig. 6. Total field in a 1.25 in. bore resulting from a 100 kG superconducting coil surrounding a water-cooled insert absorbing various amounts of power. Curve 2 assumes no limitation of stress, and curve 1 shows the effect of stress limiting in the water-cooled insert.

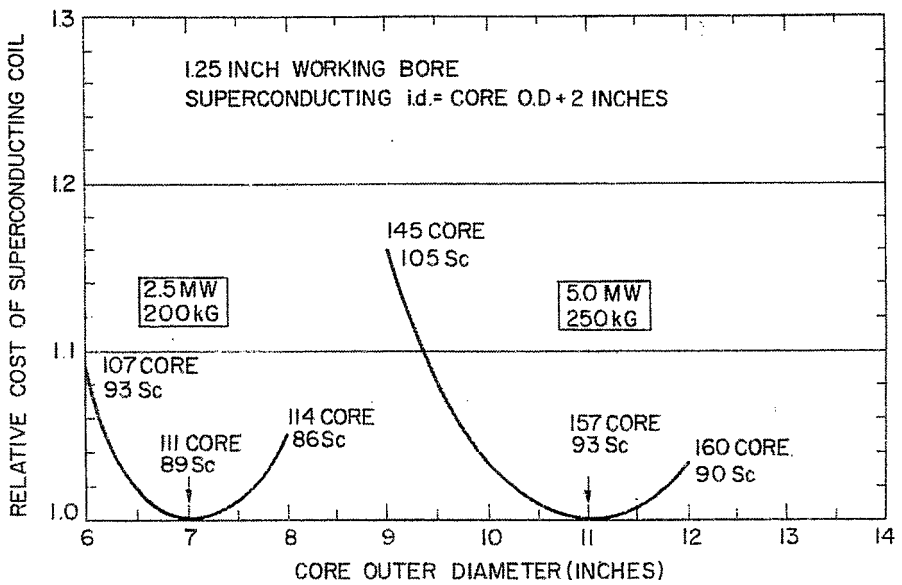

Fig. 7. Relative cost of superconducting outer coils as a function of the outer diameter of the insert core. The superconducting coils are assumed to be 2 in. larger than the core o.d. (see text).

Fig. 8. A typical 5 MW water-cooled insert (Ref. 5) consisting of two coils, the inner producing 75 kG and the outer 100 kG. The clearance dimension outside the containing barrel is 14 in.

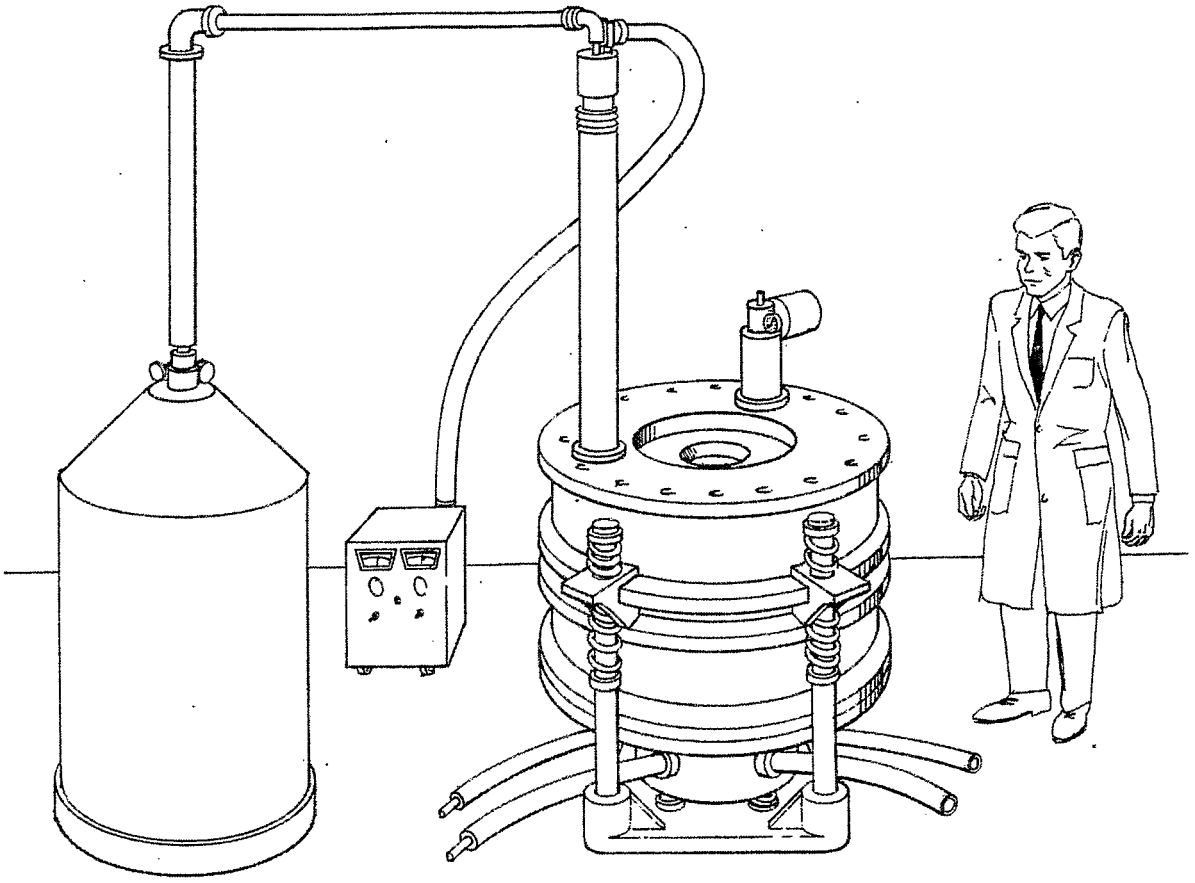

Fig. 9. Over-all view of the 225 kG hybrid water-cooled and superconducting magnet system being developed at the Francis Bitter National Magnet Laboratory. The external helium storage vessel is at the left and supplies helium to the magnet cryostat. The 8 kW power supply is shown between the cryostats. A small refrigerator is shown mounted on top of the magnet cryostat and is used to hold the magnet at 20°K between scheduled operations. The magnet cryostat is mounted on heavy springs to allow relative motion between the two coil systems under fault conditions.

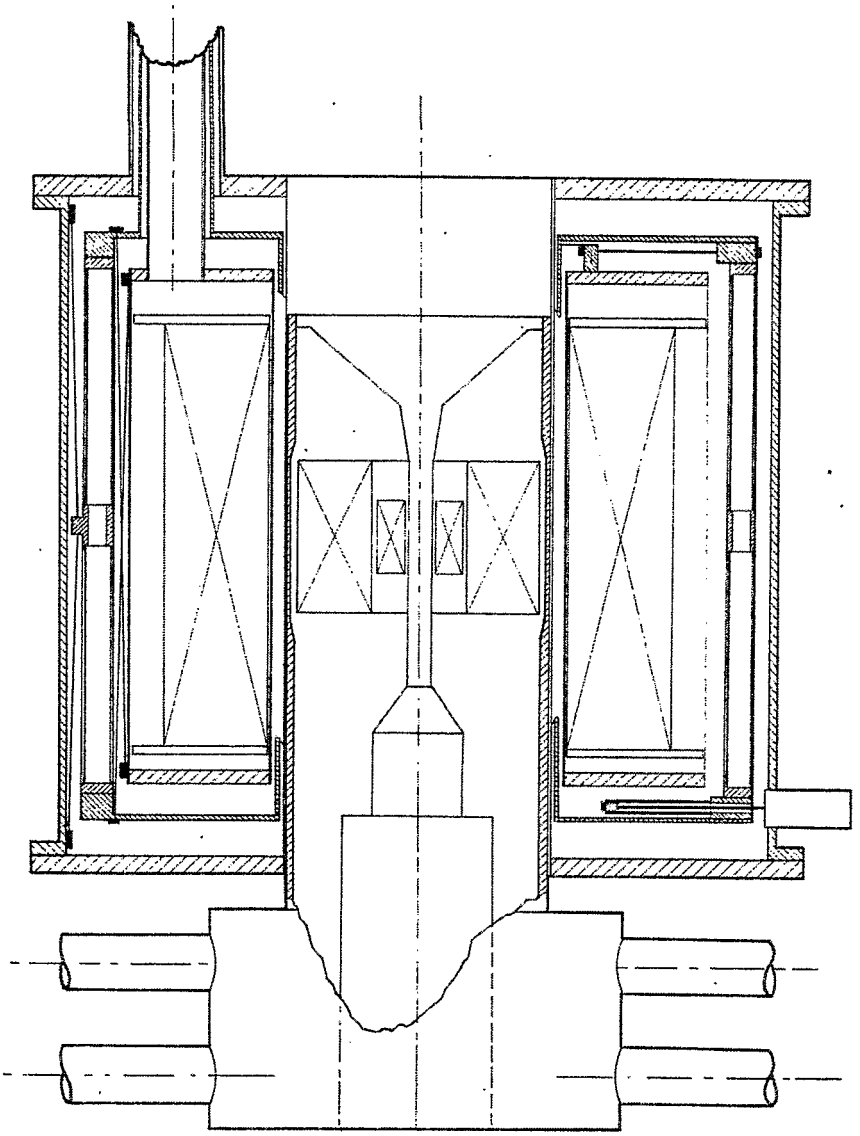

Fig. 10. Schematic of the 225 kG hybrid magnet. A pair of water-cooled coils consuming 5 MW of dc power are to be operated inside a 14 in. room temperature bore 60 kG superconducting coil. The superconducting coil will weigh 1600 lb and store 2 MJ of energy. The helium Dewar containing the coil as well as the nitrogen shield Dewar are suspended against the very large magnetic interaction forces by the spokes indicated schematically in the left-hand section. Access for electrical leads and cryogenic fluids is provided through the 3 in. neck tube shown at the top left of the cryostat. The water-cooled insert can be exchanged easily for alternate cores without disturbing the superconducting coil. All water and power connections for the water-cooled section are located below the insert.

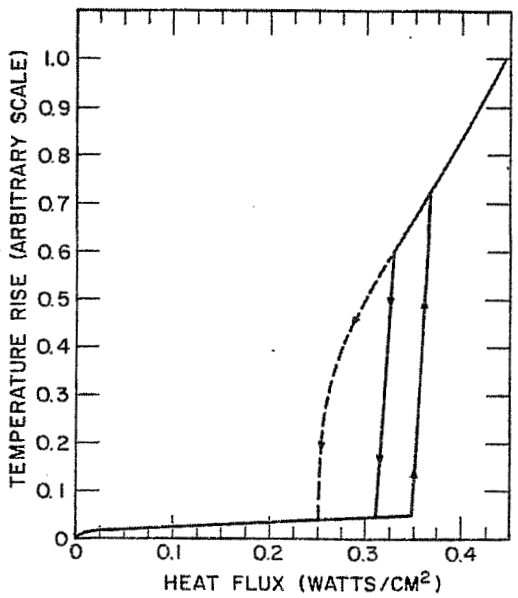

Fig. 11. Critical heat flux measurements in passages simulating those in the magnet, 0.017 in. high by 0.3 in. wide by 0.397 in. long. The dotted curve results when a large input of bubbles is produced with a heater below the test section, simulating a normal zone in a lower pancake.

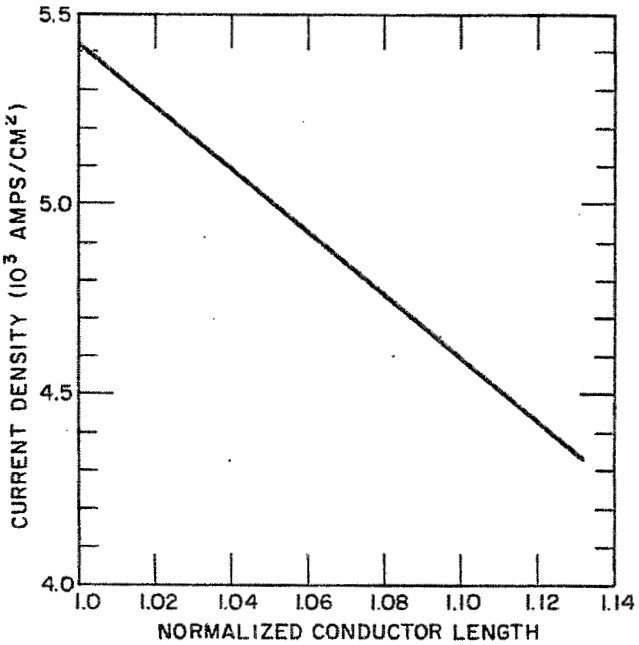

Fig. 12. Effect on conductor length of changing passage height and consequently the turns/cm^2 and the over-all current density at fixed current.

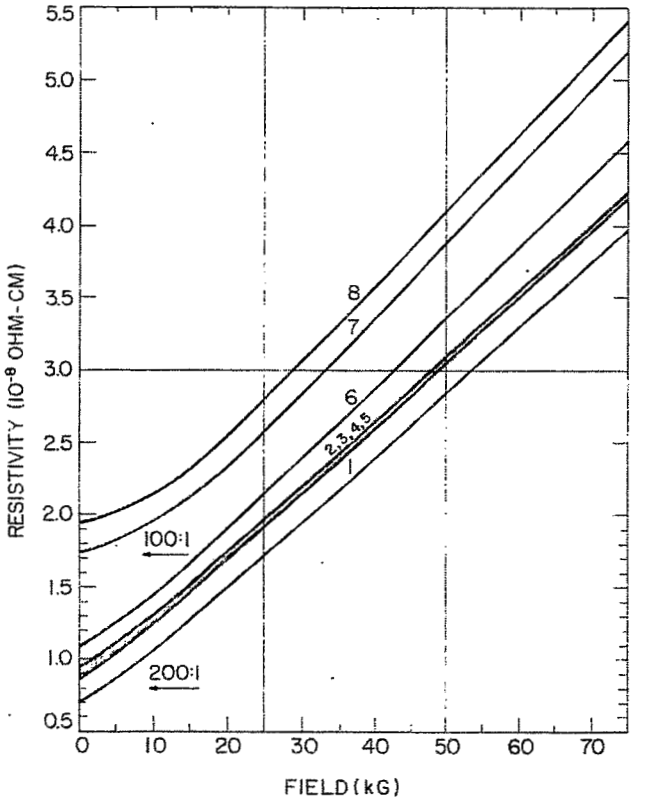

Fig. 13. Effect of magnetoresistance on a variety of composite samples of different initial resistivities. Curves 1 and 2 and 7 and 8 before and after strain, illustrating the simple additive nature of the two resistivity contributions.

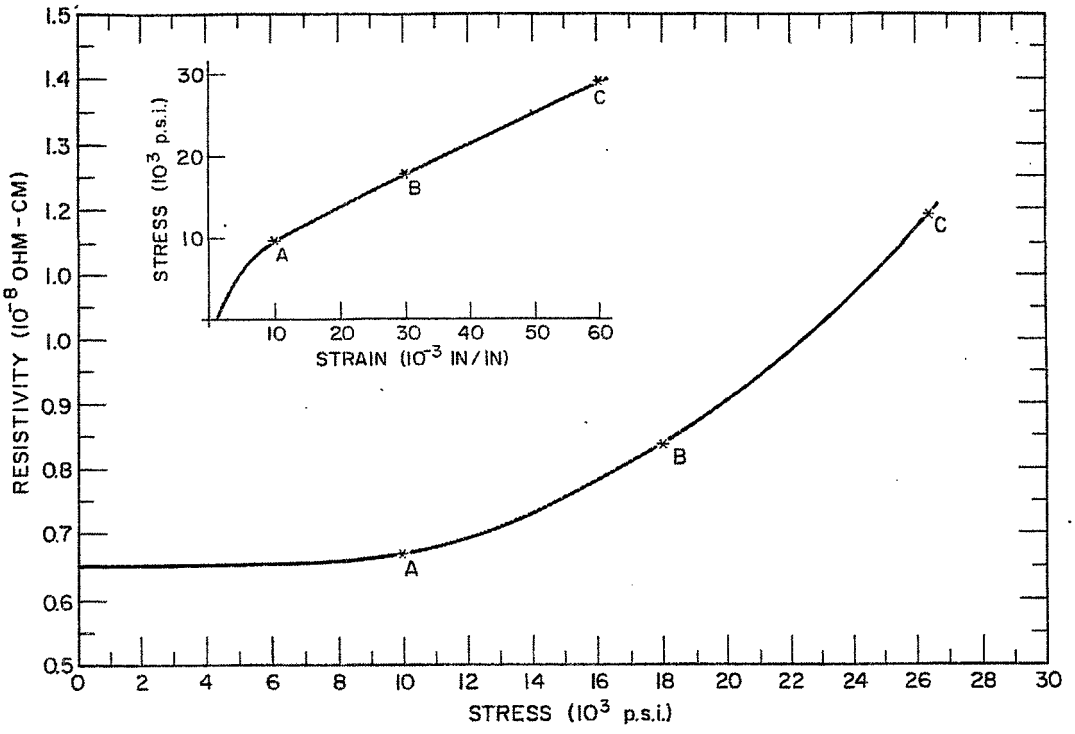

Fig. 14. Effect of stress and strain on the resistivity of copper magnet wire. A 1% strain is required before any effect on resistivity is noted.

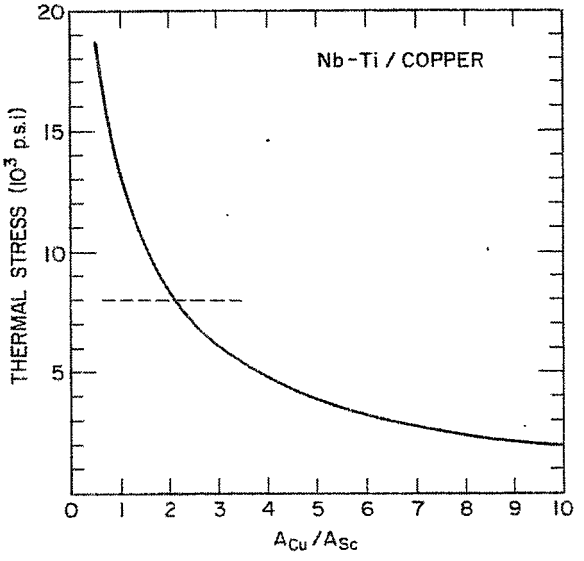

Fig. 15. Thermal stress induced in the copper portion of a copper-NbTi composite conductor as a function of the area ratio of copper to superconductor (see text).

$$(1)\quad \omega_s = h_0 \Delta T^n$$

$$(2)\quad \Delta T = \left(\frac{I_R}{I_c} \cdot \frac{I}{I_c} \frac{\rho}{APh} I_c^2 \right)^{1/n} = i_R \cdot i \cdot \alpha_n$$

$$(3)\quad \boxed{\alpha_n = \frac{I_c^2 \frac{\rho}{A}}{Ph_0 (T_c - T_b)^n}}$$

$$(4)\quad \Delta T g_s = \frac{\left(\frac{I_R}{I_c} \cdot \frac{\rho}{A} \right) \frac{I_s}{I_c} \cdot I_c^2}{8\pi k N} = i_R \cdot i_s \cdot \beta_n$$

$$(5)\quad \boxed{\beta_n = \frac{I_c^2 \frac{\rho}{A}}{8\pi k N \ (T_c - T_b)}}$$

$$(6)\quad \boxed{\beta_n i_R^2 + i_R (1 - \beta_n i) - \alpha_n i_R^{1/n} \cdot i^{1/n} + 1 - i = 0}$$

Fig. 16. Formulation used to describe the stability of copper-superconductor compounds (see text).

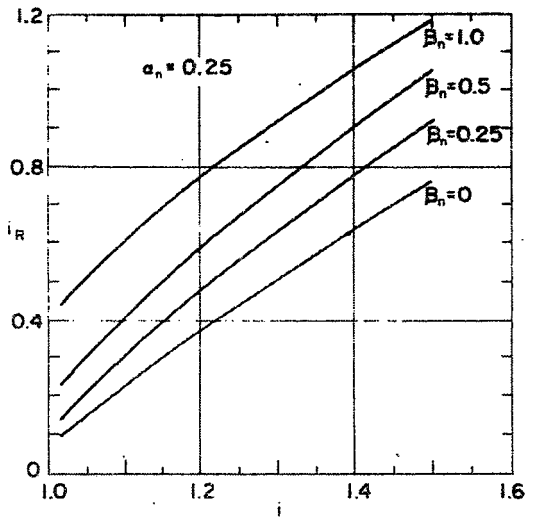

Fig. 17. Plot of Eq. (6) with $\beta_n = 0$, thus illustrating the effect of a nonlinear heat transfer in producing a discontinuity at the critical current. The normalized current, i, is the total current normalized to the critical current, $I_c(H)$, and i_R is the current in the normal path normalized to $I_c(H)$.

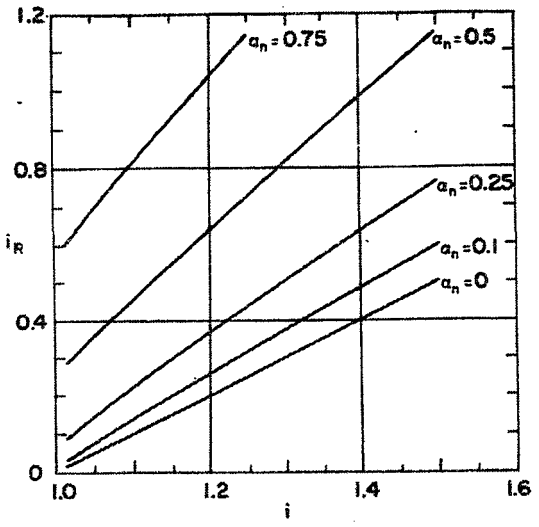

Fig. 18. Plot of Eq. (6) with $\alpha_n = 0.25$, thus illustrating the effect of a gradient within the superconducting core on discontinuities at the critical current. The normalized currents, i and i_R, are defined in Fig. 17.

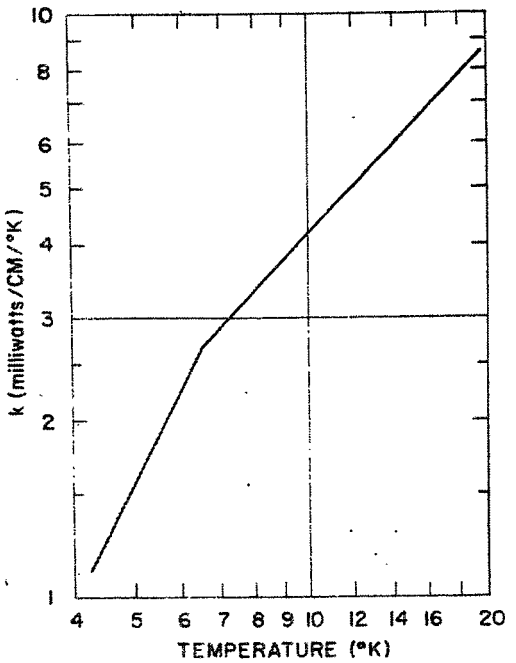

Fig. 19. Thermal conductivity of NbTi (Ref. 15) as a function of temperature at zero field. The sample consists of 19 parallel strands of 0.020 in. diameter NbTi. The measurements were made along the wire in a high vacuum cryostat.